Watermarking technique based on DWT associated with embedding rule

Jih Pin Yeh, Che-Wei Lu, Hwei-Jen Lin, and Hung-Hsuan Wu

***Abstract*—**Information hiding has been an important research topic for the past several years. Techniques to solve the problem of unauthorized copying, tampering, and multimedia data delivery through the internet are urgently needed. Today's information hiding techniques consist mainly of steganography and digital watermarking. In this paper, we shall focus on the digital watermarking and propose an improved version of the integer discrete wavelet transform (integer-DWT)-based watermarking technique proposed by Chang et al. [17]. Our method is able to achieve ownership protection. First, the original image is performed with the Discrete Wavelet Transformation (DWT) and embedded with the watermark in the HL and LH blocks associated with an embedding rule.

The experimental results show that the proposed approach indeed produces better results than the compared method in terms of the quality of the stego image, the extracted watermark with or without attack, and time efficiency.

***Keywords*—**watermarking, steganography, discrete wavelet transform (DWT), embedding rule.

I. Introduction

With the rapid development of CDROM and internet, more and more digital media such as images, videos, audios are widely distributed. However, unrestricted copying and malicious tampering cause huge financial losses and problems for intellectual property rights. Therefore, information hiding has become an important research area [1]-[4]. Information hiding techniques consist mainly of steganography [5]-[9] and digital watermarking [10]-[17].

Steganography requires the quality of the stego image to be as high as possible and the amount of embedded information to be as much as possible; while digital watermarking requires perceptual invisible (or transparency), difficult to remove without seriously affecting the image quality and robust against image attacks.

Manuscript received June 5, 2010: Revised version received July 16, 2010. This work was supported by the National Science Council of Taiwan, R. O. C. under the grant NSC-98-2221-E-032-034.

Jih Pin Yeh is with the Department of Information Management, Chinmin Institute of Technology, Miaoli County, Taiwan R.O.C. (e-mail: 891190125@s91.tku.edu.tw)

Che-Wei Lu is with the Department of Computer Science and Information Engineering, Tamkang University, Taipei, Taiwan, R.O.C. (e-mail: tony492190813@yahoo.com.tw)

Hwei-Jen Lin is with the Department of Computer Science and Information Engineering, Tamkang University, Taipei, Taiwan, R.O.C. (corresponding author to provide phone: +886-2-26215656 ext. 2738; e-mail: hjlin@cs.tku.edu.tw)

Hung-Hsuan Wu is with the Department of Computer Science and Information Engineering, Tamkang University, Taipei, Taiwan, R.O.C. (e-mail: joseph5@gmail.com).

In this paper, we shall focus on digital watermarking. Watermarking schemes can be categorized into visible and invisible ones. The latter are more popular and are further categorized into robust and fragile watermarks. Robust watermarking schemes must be able to extract the watermark after one or more of a variety of attacks. After an attack and when the watermark has been extracted, the watermark should be as correlated as highly as possible with the original watermark. Contrary to a robust watermark, fragile watermarks become totally deformed after even the slightest modification of the media, and are used mainly for authentication purposes. In addition, there are two common schemes of performing watermarking: one in spatial domain, and the other in transformed domain. In the spatial domain, the watermark is embedded into the host image by directly modifying the pixel value of the host image. On the other hand, transformed domain watermarking schemes perform the domain transformation procedure by transformation functions such as Discrete Cosine Transformation (DCT), Discrete Wavelet Transformation (DWT), Discrete Fourier Transformation (DFT),…, etc. Then, the transformed frequency coefficients are modified to embed watermark bits. Finally, the inverse of the corresponding transformation function is performed.

Several watermarking schemes have been proposed in the literature. Fu et al. [10] proposed a novel oblivious color image watermarking scheme based on Linear Discriminant Analysis (LDA). The watermark accompanied with a reference is embedded into the RGB channels of color images. By applying the embedded reference watermark, a linear discriminant matrix is obtained. The watermark can be correctly extracted under several different attacks. Bhatnagar et al. [11] proposed a new semi-blind reference watermarking scheme based on DWT and singular value decomposition (SVD) for copyright protection and authenticity. Chen et al. [12] proposed a fragile watermarking scheme based on fuzzy c-means (FCM), which used the dependency of the image blocks embedded with watermark to gain the authentication data and find the tampered position when the image was attacked by tampering or vector quantization (VQ). Yen et al. [13] presented a watermarking technique based on support vector machines (SVMs). According to the precise characteristics of the SVM, which is able to generate an optimal hyperplane for the given training samples, the requirements of imperceptibility and robustness of the watermarks are fulfilled and optimized. Yen et al. [14] proposed a novel digital watermarking technique based on SVM and Tolerable Position Map (TMP). The purpose of SVMs is two folds in this study. One is using SVM to identify tolerable embedding positions, and the other is using SVM to embed and extract watermarks. Shieh et al. [15] proposed an innovative watermarking scheme based on genetic algorithms (GA) in the

transform domain to optimize robustness and invisibility. Their simulation results showed both robustness under attacks and improvement in watermarked image quality. Rezazadeh et al. [16] applied a morphological binary wavelet transform along with a HVS (human visual system) model for watermark casting in wavelet domain. The significant parts of the decomposed watermark are embedded in lower-frequency area while its details are inserted in higher-frequency area. Using the morphological binary form of decomposed watermark allows a robust watermark recovery. Chang et al. [17] proposed a multipurpose method where the authentication watermark and the ownership watermark are embedded in the wavelet transform domain. Through a series of experiments, supportive evidence is provided to demonstrate the proposed method being effective in image authentication and pre-empting image processing attacks. However, randomly selecting the embedded blocks and taking the integer parts of DWT coefficients resulted in the PSNR decreasing.

In this paper, we propose a novel scheme to improve the method presented by Chang et al. [17]. We apply DWT instead of integer-DWT and use fixed positions instead of randomly selected positions to embed watermark. The proposed method has been shown to outperform the one presented by Chang et al. in terms of quality of stego images, robustness of watermarks, and time efficiency.

The remainder of this paper is organized as follows. Section 2 describes the details of the proposed scheme. In Section 3, the experimental results are provided to demonstrate the effectiveness of the proposed scheme. Other applications of the proposed method are shown in Section 4. Finally, conclusions are drawn in Section 5.

II. The Proposed Scheme

In 2006, Chang et al. [17] presented a multipurpose watermarking method based on integer-DWT. However, the integer-DWT is not so precise in computation that the quality of stego image is reduced. Besides, embedding watermarks into randomly selected positions in the HL and LH subbands might cause some watermark bits being embedding in the same corresponding position in the original image and result in erroneous extracted watermark. To overcome these problems, our proposed scheme is based on general DWT instead due to its accurate computation so as to enhance quality of stego image and embeds the watermark bits in the blocks located at the even columns in the HL region and the blocks located at the odd columns in the LH subband. A watermark bit is embedded according to an embedding rule. For extracting the watermarks, the same embedding rule should be referred. The details of the proposed method are described in the following.

First, we apply 1-Level DWT in the host image and divide the HL and LH subband into non-overlapping blocks of size 2*2. The watermarks are then embedded in the blocks located at the even columns of the HL subband and the blocks located at the odd columns of the LH subband as shown in Fig. 1. A watermark bit is embedded in a block by modifying the four coefficients in the block according to an embedding rule. To embed a watermark bit w in a block of size 2*2, the mean value *mean* of the four coefficients is first calculated. Let r be an integers such that $3r \le mean < 3(r+1)$, then each of the four coefficients is modified by adding a common value so that the mean of the modified coefficients equals $3r$ if ($w = 0$ and r is even) or ($w = 1$ and r is odd), and equals $3(r+1)$ if ($w = 0$ and r is odd) or ($w = 1$ and r is even). This modification causes the mean value becoming the even or odd multiple of 3 closest to the original mean value depending on the embedded watermark bit $w = 0$ or 1. As the example illustrated in Fig. 2, the mean value is between 0 and 3, then the coefficients will be modified so that the new mean value becomes 0 if $w = 0$; and 3 if $w = 1$. Finally, the IDWT (inverse DWT) is performed to form a stego image.

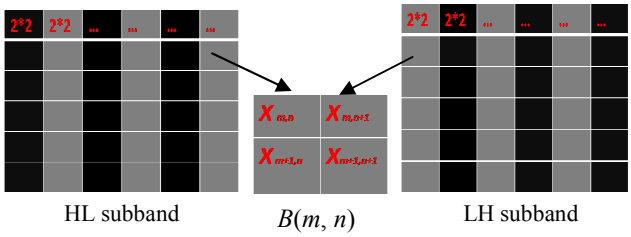

Fig. 1 Blocks selected for embedding are marked in gray. (a) Blocks in even columns of HL region are selected; (b) Blocks in odd columns of LH region are selected.

The embedding process is described as follow:

Step 1. Apply 1-Level DWT on an $M*N$ host image.

Step 2. Divide the HL and LH subband into non-overlapping blocks of size 2*2 and select blocks in even columns of HL and blocks in odd columns of LH for embedding watermark.

Step 3. For each selected block $B(m, n)$ and a watermark bit w.

//Calculate mean value $M(m, n)$ of four coefficients in $B(m, n)$

$$M(m, n) := \frac{1}{4}\left(\sum_{i=0}^{1}\sum_{j=0}^{1} x_{m+i,n+j}\right) \qquad (1)$$

//Embed watermark bit w

$R := M(m, n) \bmod 6;$

for $i := 0$ **to** 1

for $j := 0$ **to** 1

if $0 \le R < 3$ **then**

if $w = 1$ **then** $x_{m+i,n+j} := x_{m+i,n+j} + (3-R)$;

if $w = 0$ **then** $x_{m+i,n+j} := x_{m+i,n+j} - R$;

if $3 \le R < 6$ **then**

if $w = 1$ **then** $x_{m+i,n+j} := x_{m+i,n+j} + (3-R)$;

if $w = 0$ **then** $x_{m+i,n+j} := x_{m+i,n+j} + (6-R)$;

Step 4. Perform IDWT on the embedded image to obtain a stego image.

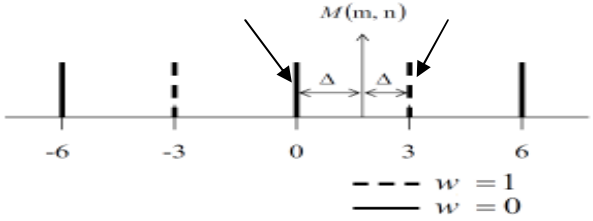

Fig. 2 Example: Block values are adjusted s. t. $M(m, n) = 0$ if $w = 0$, and $M(m, n) = 3$ if $w = 1$.

The extracting process is described as follows:

Step 1. Apply 1-Level DWT on an $M*N$ stego image.
Step 2. Divide the HL and LH subband into non-overlapping blocks of size 2*2 and select blocks in even columns of HL and blocks in odd columns of LH for extracting watermark.
Step 3. For each block $B(m, n)$
//Calculate mean value $M(m, n)$ of four coefficients in $B(m, n)$

$$M(m,n) := \frac{1}{4}\left(\sum_{i=0}^{1} \sum_{j=0}^{1} x_{m+i,n+j} \right)$$

//Extract watermark bit w
$R := M(m, n) \bmod 6$;
if $0 \le R < 1.5$ **then** $w := 0$;
if $1.5 \le R < 4.5$ **then** $w := 1$;
if $4.5 \le R < 6$ **then** $w := 0$;

III. Experimental Results

The experiments are implemented in an environment using the Intel Core 2 Duo 1.83GHz CPU, 1.99G RAM, and Microsoft XP. Test data include 100 gray-scale images of size 256*256 were used as host images and 10 binary images of size 64*64 as watermark images. Six test host images and two watermarks are selected from the data set and shown in Fig. 3. To compare the performance, the value of *PSNR* (peak signal to noise ratio) of the stego image and the value of the *NC* (normalized correlation) of the extracted watermark are evaluated. The formulae for *PSNR* and *NC* are given in (3) and (4), respectively, where H_0 and W_0 denote the height and the width of the watermark, and $w(i, j)$ and $w'(i, j)$ denote the bit values at position (i, j) of the original watermark and extracted watermark, respectively. The *MSE* (mean square error) used in the formula for *PSNR* is defined in (2), where H and W denote the height and width of the image. In general, a *PSNR* value greater than 30 dB is perceptually acceptable, and an *NC* value greater than 0.60 is conspicuous. Because Chang's method used randomly selected blocks to embed watermark, the experiment performed each set of data five times and took the average of the *PSNR* values and the average of the *NC* values. Fig.s 5 and 6 show some tested results by the method proposed by Chang et al. [17] and our method. Tables 1-3 compare the *PSNR* values of the stego images and the *NC* values of the extracted watermarks under a variety of attacks for the two methods. The comparison shows that the proposed method requires less run time and resists all the attacks listed in the table, even is better than the method proposed by Chang et al.

$$MSE = \frac{1}{W \times H} \sum_{i=1}^{H} \sum_{j=1}^{W} ((I(i,j) - I'(i,j))^2 \qquad (2)$$

$$PSNR = 10 \times \log_{10}(255^2 / MSE) \qquad (3)$$

$$NC = \sum_{i=1}^{Ho} \sum_{j=1}^{Wo} w(i,j) \times w'(i,j) / (H_0 \times W_0) \qquad (4)$$

(a) Host image F_1 (b) Host image F_2 (c) Host image F_3 (d) Host image F_4

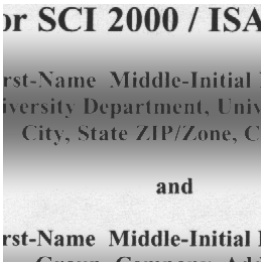

(e) Host image F_5 (f) Host image F_6 (g) watermark w_1 (h) watermark w_2

Fig. 3 Six host images and two watermarks

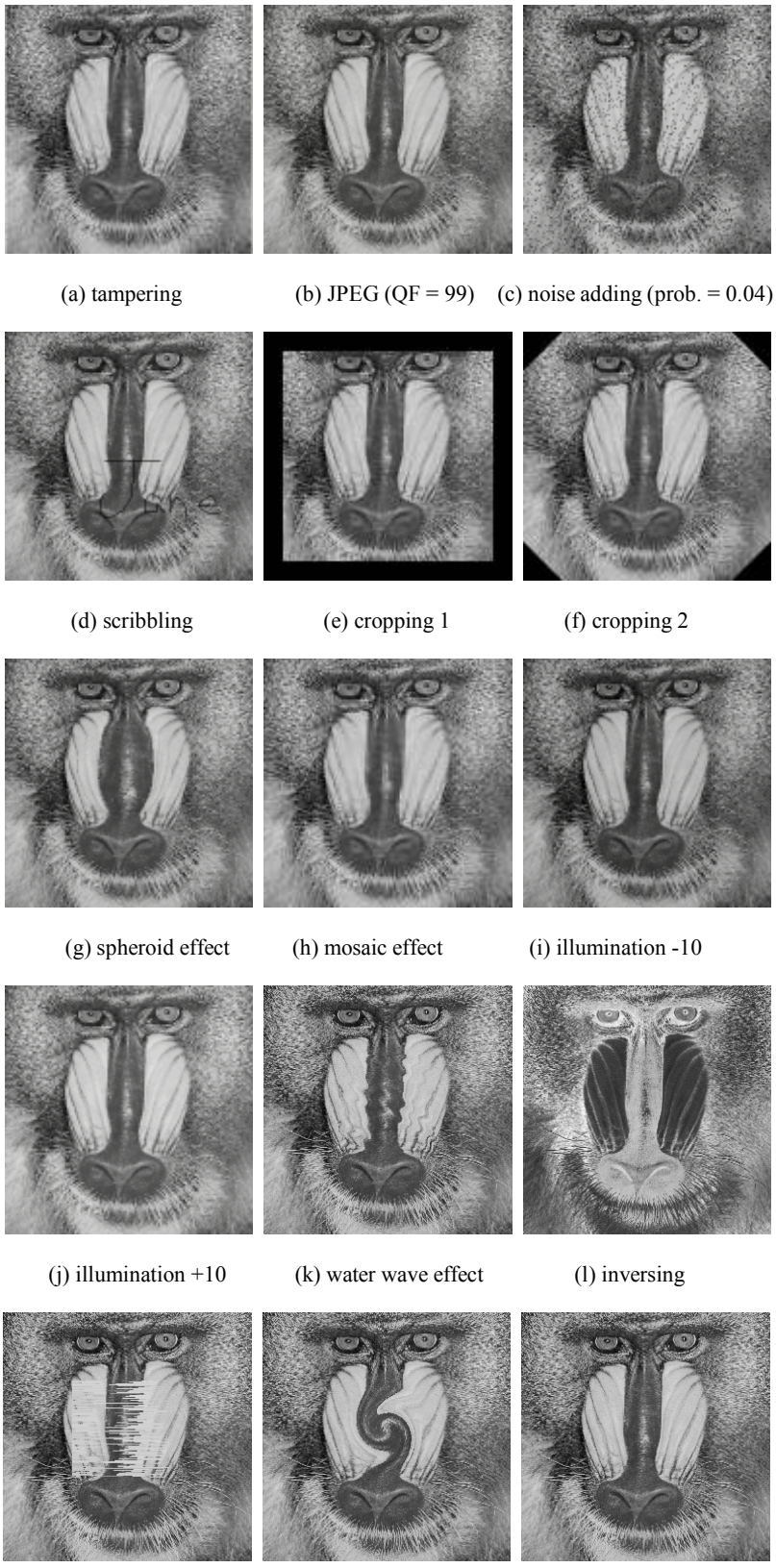

(a) tampering (b) JPEG (QF = 99) (c) noise adding (prob. = 0.04)

(d) scribbling (e) cropping 1 (f) cropping 2

(g) spheroid effect (h) mosaic effect (i) illumination -10

(j) illumination +10 (k) water wave effect (l) inversing

(m) wind effect (n) vortex effect (o) sharpening

Fig. 4 Attacked results of host image F_1

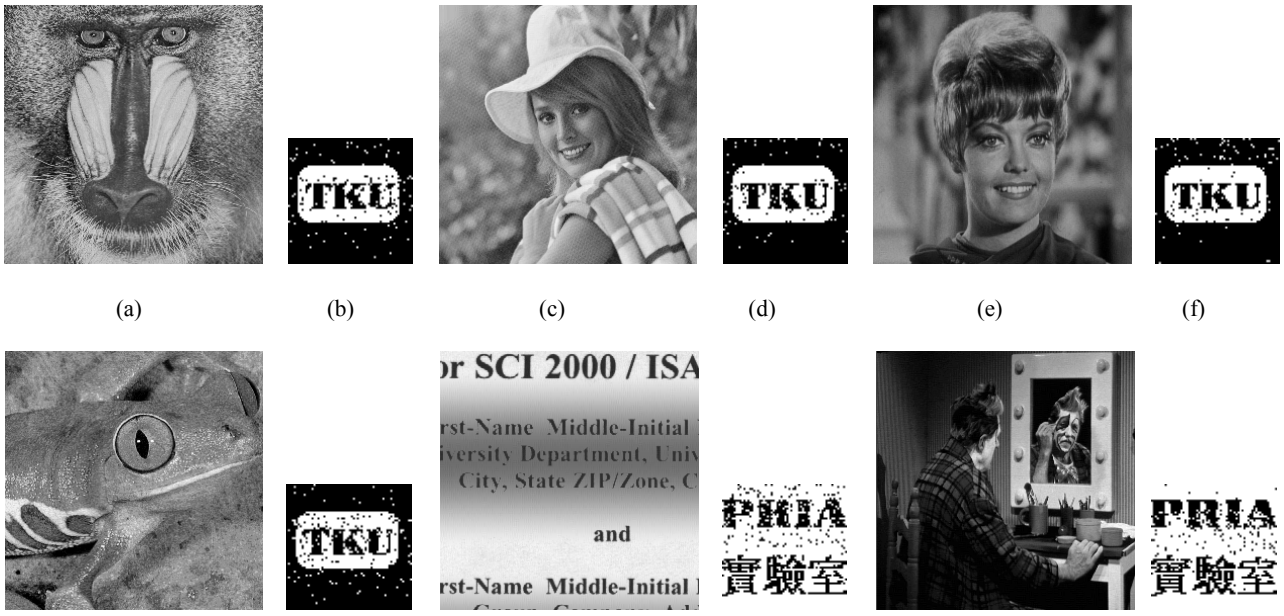

(a) (b) (c) (d) (e) (f)

(g) (h) (i) (j) (k) (l)

Fig. 5 Results of Chang's method: left column: watermarked images, right column: extracted watermarks

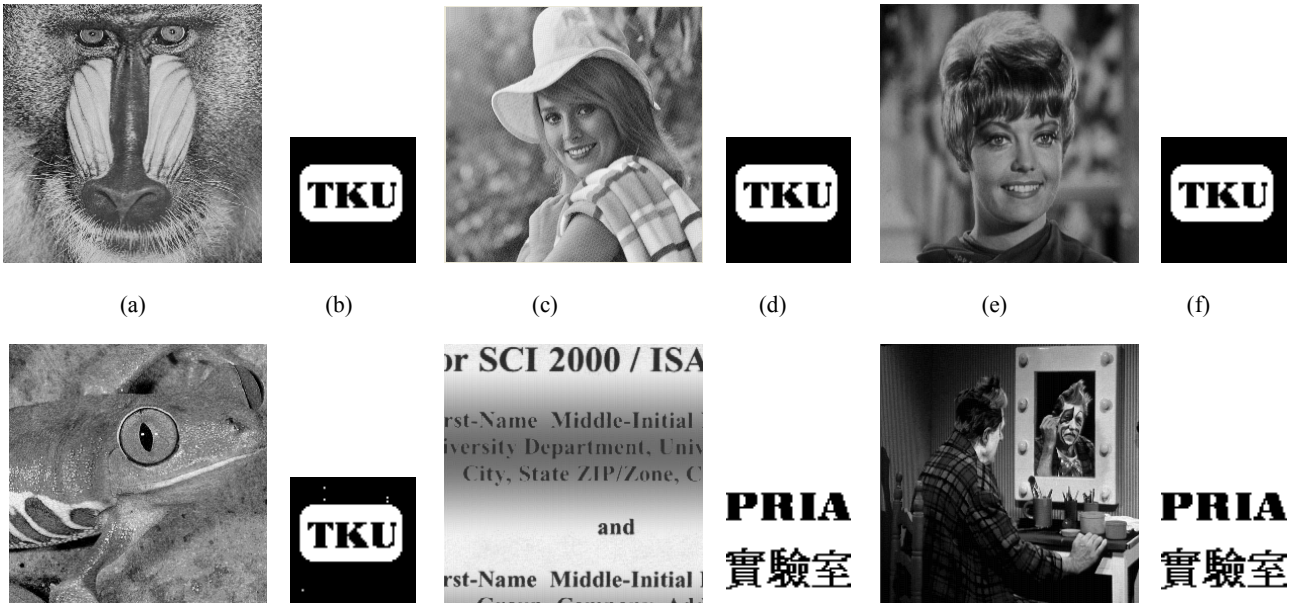

(a) (b) (c) (d) (e) (f)

(g) (h) (i) (j) (k) (l)

Fig. 6 Results of our method: left column: watermarked images, right column: extracted watermarks

Table 1. The run time, *PSNR*, *NC* with/without attacks for the two methods

Host images				
Attacks\Methods	Chang's method	our method	Chang's method	our method
time(embedding & extracting)	5 sec.	3 sec.	5 sec.	3 sec.
PSNR	41.74	43.24	42.11	43.54
NC (unattacked)	0.93	1.00	0.95	1.00
NC (noise adding, prob. = 0.01)	0.73	0.75	0.68	0.73
NC (noise adding, prob. = 0.02)	0.63	0.67	0.60	0.62
NC (cropping 1)	0.78	0.88	0.80	0.88
NC (cropping 2)	0.91	0.98	0.92	0.98
NC (scribbling)	0.93	0.97	0.93	0.98
NC (tampering)	0.91	0.96	0.94	0.99
NC (JPEG QF = 99)	0.94	1.00	0.94	1.00
NC (JPEG QF = 96)	0.92	1.00	0.93	1.00
NC (JPEG QF = 93)	0.82	0.94	0.85	0.95
NC (JPEG QF = 90)	0.66	0.78	0.70	0.83
NC (JPEG QF = 87)	**0.49**	0.60	**0.57**	0.65
NC (illumination +10)	0.94	1.00	0.95	1.00
NC (illumination -10)	0.94	1.00	0.95	1.00
NC (contrast +10)	0.74	0.85	0.88	0.98
NC (contrast -10)	0.81	0.89	0.93	0.98
NC (illumination, contrast +20)	**0.39**	**0.43**	0.67	0.77
NC (water wave effect)	0.81	0.84	0.81	0.87
NC (wind effect)	0.83	0.88	0.84	0.91
NC (vortex effect)	0.83	0.88	0.84	0.89
NC (sharpening)	0.93	1.00	0.95	1.00
NC (inversing)	0.94	1.00	0.94	1.00
NC (mosaic effect)	0.82	0.84	0.83	0.87
NC (spheroid effect)	0.82	0.87	0.83	0.87

Table 2. The run time, *PSNR*, *NC* with/without attacks for the two methods

Host images			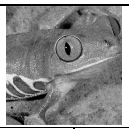	
Attacks\Methods	Chang's method	our method	Chang's method	our method
time(embedding & extracting)	5 sec.	3 sec.	5 sec.	3 sec.
PSNR	42.09	43.68	42.00	43.19
NC (unattacked)	0.95	1.00	0.91	1.00
NC (noise adding, prob. = 0.01)	0.66	0.69	0.67	0.71
NC (noise adding, prob. = 0.02)	**0.57**	**0.59**	**0.57**	0.62
NC (cropping 1)	0.80	0.88	0.78	0.88
NC (cropping 2)	0.91	0.98	0.88	0.98
NC (scribbling)	0.93	0.98	0.89	0.98
NC (tampering)	0.92	0.99	0.90	0.99
NC (JPEG QF = 99)	0.94	1.00	0.91	1.00
NC (JPEG QF = 96)	0.92	1.00	0.89	0.99
NC (JPEG QF = 93)	0.84	0.96	0.80	0.94
NC (JPEG QF = 90)	0.72	0.83	0.64	0.78
NC (JPEG QF = 87)	0.60	0.68	**0.45**	**0.58**
NC (illumination +10)	0.95	1.00	0.91	1.00
NC (illumination -10)	0.94	1.00	0.89	0.98
NC (contrast +10)	0.90	0.99	0.79	0.94
NC (contrast -10)	0.94	1.00	0.86	0.95
NC (illumination, contrast +20)	0.72	0.85	**0.42**	**0.55**
NC (water wave effect)	0.83	0.86	0.76	0.84
NC (wind effect)	0.85	0.89	0.77	0.85
NC (vortex effect)	0.86	0.90	0.80	0.89
NC (sharpening)	0.95	1.00	0.91	1.00
NC (inversing)	0.95	1.00	0.91	1.00
NC (mosaic effect)	0.83	0.84	0.79	0.85
NC (spheroid effect)	0.85	0.89	0.79	0.88

Table 3. The run time, *PSNR*, *NC* with/without attacks for the two methods

Host images	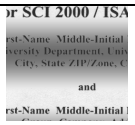			
Attacks\Methods	Chang's method	our method	Chang's method	our method
time(embedding & extracting)	5 sec.	3 sec.	5 sec.	3 sec.
PSNR	40.77	41.77	41.48	42.02
NC (unattacked)	0.87	1.00	0.91	1.00
NC (noise adding, prob. = 0.01)	0.60	0.70	0.74	0.79
NC (noise adding, prob. = 0.02)	**0.51**	0.60	0.64	0.70
NC (cropping 1)	**0.52**	**0.51**	**0.54**	**0.51**
NC (cropping 2)	0.81	0.90	0.84	0.90
NC (scribbling)	0.85	0.98	0.89	0.98
NC (tampering)	0.84	0.96	0.91	0.99
NC (JPEG QF = 99)	0.88	1.00	0.91	1.00
NC (JPEG QF = 96)	0.86	1.00	0.88	1.00
NC (JPEG QF = 93)	0.77	0.97	0.78	0.96
NC (JPEG QF = 90)	0.65	0.83	0.65	0.85
NC (JPEG QF = 87)	**0.56**	**0.46**	**0.49**	0.66
NC (illumination +10)	0.88	1.00	0.91	1.00
NC (illumination -10)	0.87	1.00	0.62	0.64
NC (contrast +10)	0.68	0.88	**0.55**	**0.59**
NC (contrast -10)	0.79	0.89	0.88	0.93
NC (illumination, contrast +20)	**0.20**	**0.20**	**0.55**	0.70
NC (water wave effect)	0.74	0.85	0.77	0.85
NC (wind effect)	0.81	0.92	0.80	0.88
NC (vortex effect)	0.74	0.87	0.80	0.89
NC (sharpening)	0.87	1.00	0.91	1.00
NC (inversing)	0.86	1.00	0.91	1.00
NC (mosaic effect)	0.68	0.78	0.72	0.83
NC (spheroid effect)	0.74	0.83	0.78	0.87

IV. Other Applications

Our method can also be applied on watermarking in color images. The watermark is embedded into the blue channel due to the fact that human eyes are less sensitive to blue channel. The embedding and extracting processes are the same as that for watermarking in gray-scale images. In the experiments, we use 100 color images of size 256*256 as host images and 10 binary images of size 64*64 as watermark. Four test host images and one watermark are selected from the data set and shown in Fig. 7. To compare the performance, the value of *PSNR* of the stego image and the value of the *NC* of the extracted watermark are evaluated. The *MSE* used for evaluating the *PSNR* value for color stego images is different from that for gray-scale stego images. It is given in (5). To test the robustness of the proposed method we tested on a variety of attacks. Fig. 8 shows some tested results by our method. Table 4 shows the *NC* value of four host images under a variety of attacks for our method. Experimental results show the quality of watermarked images and the extracted watermarks with/without attacks and attacks are satisfactory. To test the robustness of the proposed method we tested on a variety of attacks. Fig. 8 shows some tested results by our method. Table 4 shows the *NC* value of four host images under a variety of attacks for our method. Experimental results show the quality of watermarked images and the extracted watermarks with/without attacks and attacks are satisfactory.

$$MSE=\sum_{i=1}^{H}\sum_{j=1}^{W}((R_{ij}-\bar{R}_{ij})^2+(G_{ij}-\bar{G}_{ij})^2+(B_{ij}-\bar{B}_{ij})^2)/(3\times H\times W) \quad (5)$$

(a) Host image F_7

(b) Host image F_8

(c) Host image F_9

(d) Host image F_{10}

(e) watermark w_1

Fig. 7 Four host images and one watermark

(a)

(b)

(c)

(d)

(e)

(f)

(g)

(h)

Fig. 8 Results of our method: left column: watermarked images, right column: extracted watermarks

Table 4. The *PSNR*, *NC* with/without attacks for our method tested on color images

Attacks\Host images	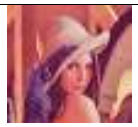			
PSNR	48.49	48.61	48.79	48.36
NC (unattack)	1.00	0.99	1.00	1.00
NC (noise adding prob. = 0.01)	0.78	0.71	0.86	0.75
NC (noise adding prob. = 0.02)	0.70	0.63	0.82	0.67
NC (cropping 1)	0.88	0.88	0.88	0.88
NC (cropping 2)	0.98	0.98	0.98	0.99
NC (scribbling)	0.98	0.98	0.98	0.98
NC (tampering)	0.98	0.99	1.00	1.00
NC (illumination +10)	1.00	0.99	1.00	1.00
NC (illumination -10)	1.00	0.91	1.00	0.96
NC (contrast +10)	0.98	0.88	0.97	0.85
NC (contrast -10)	0.98	0.94	0.98	0.88
NC (illumination, contrast +20)	0.82	0.75	0.70	**0.52**
NC (inversing)	1.00	0.99	1.00	1.00
NC (water wave effect)	0.87	0.87	0.90	0.87
NC (hue +10)	0.78	0.86	0.95	0.84
NC (chrominance +10)	1.00	0.94	1.00	0.99
NC (hue -10)	0.87	0.76	0.96	0.76
NC (chrominance -10)	1.00	0.97	0.97	0.98
NC (wind effect)	0.88	0.87	0.92	0.89
NC (sharpening)	1.00	0.99	1.00	1.00
NC (blurring)	0.60	**0.56**	0.60	**0.43**
NC (vortex effect)	0.90	0.90	0.91	0.89
NC (hue, chrominance +20)	0.62	0.71	0.92	**0.57**
NC (mosaic effect)	0.87	0.87	0.89	0.87
NC (spheroid effect)	0.89	0.89	0.90	0.87

V. CONCLUSION

In this paper, we propose a DWT-based image watermarking scheme associated with an embedding rule, which is an improved version of the method proposed by Chang et al. [17]. Our method improves the robustness and the quality of stego image by embedding watermarks into some fixed blocks rather than randomly selected blocks in the HL and LH subbands and using general DWT instead of integer-DWT. The experimental results show that our method requires less time cost and provides better *PSNR* values for stego images and better *NC* values for extracted compared with Chang's method watermarks with/without attacks. In the future, we would like to give some security protection for watermarks such as reshaping or visual cryptography before embedding, and try to extend the applications of our method to video.

REFERENCES

[1] C. T. Hsieh and Y. K. Wu, "Geometric Invariant Semi-fragile Image Watermarking Using Real Symmetric Matrix," *WSEAS Trans. on Signal Processing*, vol. 2, no. 5, pp. 612-618, 2006.

[2] C. T. Hsieh, Y. K. Wu, and K. M. Hung, "An Adaptive Image Watermarking System Using Complementary Quantization," *WSEAS Trans. on Information Science and Applications*, vol. 3, no. 12, pp. 2392-2397, 2006.

[3] K. M. Hung, C. T. Hsieh, and Y. K. Wu, "Multi-Purpose Watermarking Schemes for Color Halftone Image Based on Wavelet and Zernike Transform," *WSEAS Trans. on Computer*, vol. 6, no 1, pp. 9-14, 2007.

[4] K. Prayoth, A. Kitty, and S. Arthit, "An optimal robust digital image watermarking based on genetic algorithms in multiwavelet domain," *WSEAS Trans. on Signal Processing*, vol. 5, no. 1, pp. 42-51, 2009.

[5] C. C. Chang, J. Y. Hsiao, and C. S. Chan, "Finding optimal least-significant-bit substitution in image hiding by dynamic programming strategy," *Pattern Recognition Letters*, vol. 36, no. 7, pp. 1583-1595, 2003.

[6] C. H. Yang, "Inverted pattern approach to improve image quality of information hiding by LSB substitution," *Pattern Recognition Letters*, vol. 41, no. 8, pp. 2674-2683, 2008.

[7] C. C. Lee, H. C. Wu, C. S. Tsai, and Y. P. Chu, "Adaptive lossless steganographic scheme with centralized difference expansion," *Pattern Recognition Letters*, vol. 41, no. 6, pp. 2097-2106, 2008.

[8] Z. Ni, Y. Q. Shi, N. Ansari, and W. Su, "Reversible data hiding," *IEEE Trans. on Circuits and Systems for Video Technology*, vol. 16, no. 3, pp. 354-362, 2006.

[9] Y. P. Hsieh, C. C. Chang, and L. J. Liu, "A two-codebook combination and three-phase block matching based image-hiding scheme with high embedding capacity," *Pattern Recognition Letters*, vol. 41, no.10, pp. 3104-3113, 2008.

[10] Y. G. Fu and R. M. Shen, "Color image watermarking scheme based on linear discriminant analysis," *Computer Standards & Interfaces*, vol. 30, no. 3, pp. 115-120, 2008.

[11] G. Bhatnagar and B. Raman, "A new robust reference watermarking scheme based on DWT-SVD," *Computer Standards & Interfaces*, vol. 31, no. 5, pp.1002-1013, 2009.

[12] W. C. Chen and M. S. Wang, "A fuzzy c-means clustering-based fragile watermarking scheme for image authentication," *Expert Systems with Applications*, vol. 36, no. 2, pp. 1300-1307, 2009.

[13] S. H. Yen and C. J. Wang, "SVM based watermarking technique," *Tamkang Journal of Science and Engineering*, vol. 9, no. 2, pp. 141-150, 2006.

[14] S. H. Yen, C. J. Wang, and Y. T. Kao, "A watermarking scheme based on SVM and tolerable position map," in *Proc. Int. Conf. on Systems, Man, and Cybernetics*, vol. 4, 2006, pp. 3170-3175.

[15] C. S. Shieh, H. C. Huang, F. H. Wang, and J. S. Pan, "Genetic watermarking based on transform-domain techniques," *Pattern Recognition Letters*, vol. 37, no. 3, pp. 555-565, 2004.

[16] S. Rezazadeh and M. Yazdi, "An adaptive watermarking scheme based on morphological binary wavelet decomposition," in *Proc. Int. Conf. on Signal Processing*, vol. 4, 2006, pp. 16-20.

[17] C. C. Chang, W. L. Tai, and C. C. Lin, "A multipurpose wavelet-based image watermarking," in *Proc. Int. Conf. on Innovative Computing, Information and Control*, vol. 3, 2006, pp. 70-73.